

## Influence of Slice Orientations on Susceptibility Weighted Imaging in the Thalamus

Mahmoud Refaat<sup>1</sup>, Amir Eissa<sup>1</sup>, Mohamed Elsamahy<sup>2</sup> and Tamer M. Elsayed<sup>1</sup>.

<sup>1</sup>Biophysics branch, Physics Department, Faculty of Science, Al-Azhar University, Nasr City, Cairo 11884, and <sup>2</sup>Neurology Department, Faculty of Medicine, Suez Canal University, Egypt.

**T**HALAMUS is a subcortical brain structure which divided into smaller nuclei with specific functions that aid in neuronal signal transmission and regulation, it has been the subject of a lot of neurological studies and clinical therapies, traditional imaging modalities like  $T_1$  and  $T_2$ -weighted imaging provide weak contrast in the thalamus. The thalamus has been demonstrated to be a promising target for Susceptibility-weighted image (SWI). SWI is a  $T_2^*$  gradient echo sequence, which is extremely sensitive to compounds with magnetic characteristics. The phase and magnitude of SWI can aid in the diagnosis of a variety of diseases. Spatial differences in the primary magnetic field of the magnetic resonance imaging (MRI) scanner have a significant impact on phase data. When acquiring SWI in diagnostic imaging, the axial acquisition is the most common plane of alignment. Because of the relative heterogeneity in patient placement and anatomy, clinical requirements frequently lead to changes in alignment angles. The line of the anterior and posterior commissure AC-PC can change in direction regarding the transverse plane of the MRI system for many patients receiving brain MRI. We studied whether there are any major effects on SWI phase data due to oblique orientation. According to the resulting data, there were considerable changes in phase values between axial and anatomically aligned cases.

**Keywords:** MRI; SWI; Diagnostic Imaging; Slice Orientation; Deep Gray Matter; Phase Image.

### Introduction

SWI utilizes changes in tissue magnetic susceptibility, which defines the magnetic response of tissues placed in an external magnetic field, to improve image contrast in conventional MRI. A gradient-recalled echo (GRE) sequence with a comparatively lengthy echo time (TE) was used [1]. The magnetic susceptibility information is added to the brain structure using a SW image, which combines a phase image and a magnitude image. The static magnetic field inhomogeneities, which are influenced by a macroscopic and microscopic effect, are reflected in the image phase variations [2]. The macroscopic effect, also known as the geometry effect, occurs when the configuration of tissues disrupts the homogeneity of the local field, such as the white matter tract, capillary beds, and interstitial space [2]. The microscopic effect is defined as the local field's homogeneity being altered by substances with varying magnetic susceptibilities [1, 3].

Variations in tissue magnetic susceptibility are thus generated from both the tissue's geometry and the compounds' sensitivity to the applied field. The compounds of relevance can be classified into paramagnetic or diamagnetic based on their response to the applied field. Ferritin, which contains ferric iron, deoxygenated hemoglobin, and ceruloplasmin are examples of paramagnetic compounds, while myelin, calcium, and oxygenated hemoglobin are examples of diamagnetic compounds.[2]. Because of the iron, grey matter structures such as the Thalamus are paramagnetic, but the white matter is diamagnetic due to myelination[4]. In comparison, the deep grey nuclei have the highest concentrations of iron, whereas the other components are rather minor. [5]. In the brains of patients with neurodegenerative disorders, abnormal iron deposition patterns were discovered [6]. Excess iron can harm neurons by causing free radicals to form. [7]. As a result, iron accumulation is assumed to be important in

the development of neurodegenerative disorders [8-10]. The aberrant iron deposition changes the iron distribution and concentration in the brain, affecting tissue magnetic susceptibility [1]. SWI can detect changes in susceptibility by recording phase variations produced by iron deposition and multiplying the processed phase image with the magnitude image several times, which allows for increased phase contrast and indirect iron content assessment [11]. The gray matter, particularly the thalamus, has been demonstrated to be a promising target for SWI [12]. This subcortical brain structure is divided into smaller nuclei with specific functions that aid in neuronal signal transmission and regulation [13, 14]. It has been the subject of a lot of neurological studies and clinical therapies. Neuronal abnormalities in the anterior and mediodorsal nuclei, as well as the pulvinar (Pu), for example, have been associated with psychotic diseases like schizophrenia and multiple sclerosis (MS) [15, 16]. To treat essential tremors, the ventral intermediate nucleus (Vim) is frequently targeted [17], this procedure can be performed non-invasively using radiosurgery [18] or focused ultrasound [19]. However, precise, non-invasive targeting is required. Unfortunately, traditional imaging modalities like  $T_1$  and  $T_2$ -weighted imaging provide weak contrast in the thalamus, and diffusion tensor imaging cannot resolve some of its particular nuclei, such as the Vim [20]. Indirect mapping methods based on conventional atlases can help with distinction, but they don't account for individual anatomical differences. Despite the high-resolution potential of SWI, it presently faces a significant unsolved issue that could impair image quality and diagnostic utility. Because of the heterogeneity in patient anatomy and position in clinical imaging, constant anatomic alignment of the slab orientation often needs varied oblique angles. The sagittal angle of the anterior commissure and superior commissure (ACPC) line in patients, for example, can vary significantly relative to the transverse direction, with one study of 30 patients revealing a range of  $-33^\circ$  to  $+30^\circ$  with a standard deviation of  $20^\circ$  [21]. Therefore, there exists a significant variation in voxel orientation relative to the main magnetic field, as well as voxel encoding gradients played out on each physical gradient axis that can be predicted in patient studies using ACPC alignment [22]. Changes in voxel orientation may have an impact on techniques that are sensitive to magnetic dipole effects, which are highly dependent on the direction of the main magnetic

field. [23-25]. Different summation effects may result from different voxel orientations, especially when anisotropic voxels are employed. [26-28].

We used statistical analysis of SW phase image data collected from 10 patients who had undergone an MRI brain routine that included two SWI in axial orientation, one on true transverse alignment, and a second SWI aligned with the anatomical position of the anterior-posterior commissure AC-PC line, by measuring phase values from the right and left thalamus. By drawing regions of interest (ROI) around the thalamus in both the left and right hemispheres of the brain, mean and standard deviation were taken into account to see if there were any significant effects on SWI phase data due to oblique orientation, and if there were any significant differences in phase value between true axial and anatomically axial alignment.

## **Materials and Methods**

### *Patients*

In this study, after approval by a research ethics committee, Faculty of Medicine, Suez Canal University, verbal consent was obtained from all patients involved in the study. Ten patients (5 males and 5 females) with a mean age of  $44.95 \pm 17.23$  years were submitted for brain MRI as a routine checkup. The MRI in most cases was done for different clinical symptoms such as headache, tinnitus, seizures, and vertigo.

### *MRI data acquisition and analysis*

All MRI scans were acquired at MR machine 1.5 Tesla (Philips, Achieva DS, head and neck coil). Brain routine protocol included fluid-attenuated inversion recovery (FLAIR),  $T_1$ -weighted image, Diffusion-weighted image, and Susceptibility-weighted phase image (SWI). The SWI sequence parameters are field of view  $232 \times 200$ ; the size of the matrix,  $272 \times 200$ ; size of the voxel,  $0.85 \text{ mm} \times 1 \text{ mm} \times 2 \text{ mm}$ ; TE 40ms, TR 51 ms, and  $20^\circ$  flip angle with 1.5 SENSE to reduce scan time, 2 mm thickness and 130 slices. The scan time of SWI was 4 minutes. The SWI is the post-processed form of the phase and magnitude, the filtered phase ranges from  $-\pi$  to  $+\pi$ , where in the equipment used, diamagnetic products (calcifications) are hyperintense, while paramagnetic products (e.g. deoxy-hemoglobin) showing hypointense. The SWI is acquired two times for all subjects; the first time, when the slab selection was in the direction in which feet to head (FH) is parallel to the main magnetic field (zero-angle), another SWI was performed with AC-PC line (anatomy-angle) anatomical alignment.

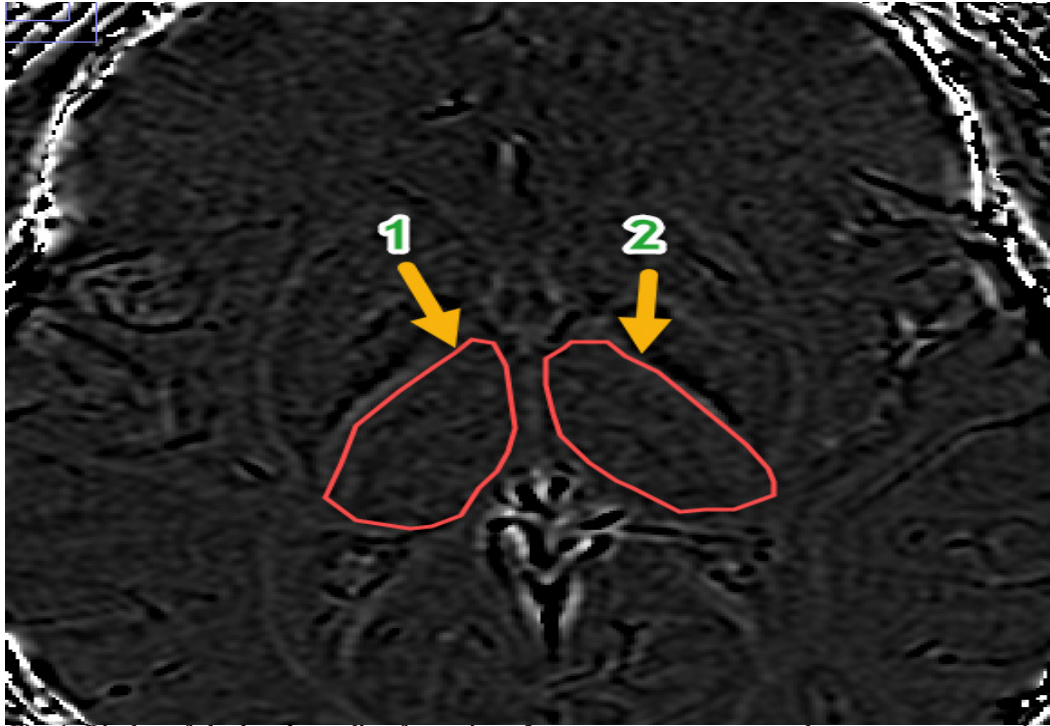


Fig. 1. Display of the basal ganglia of a patient, 2 gray matter areas were drawn as representative regions of interest with a magnification factor of 4.0. 1, 2 = bilateral Thalamus.

The regions of interest (ROI) were drawn manually and identified by using ImageJ software according to the anatomical structures[29]. The values were measured from the filtered phase images where the mean phase value of the structure was drawn. The phase values were measured from the left and right thalamus (**Figure 1**), for each ROI at least four slices are cutting through the thalamus while having a well-defined border. Furthermore, when setting the ROIs, care was taken, to avoid hypointense rim around the basal ganglia and veins cutting through the region of interest. Four measurements were done for each structure corresponding to four ROIs, and the final values of phase in milliradians were derived from the mean values of the four images.

#### *Statistical analysis*

The measured phase values were statistically analyzed by the Statistical Package for Social Science (SPSS) version 26.0. All data are presented as the mean and standard deviation.

To test the effect of alignment on SWI phase value, a paired-samples t-test was applied to the phase values of bilateral hemispheres thalamus in zero-alignment and anatomical-alignment groups respectively, a t-test is used to compare all asymmetrical regions of both groups, and evaluate,

whether there was phase difference between zero-alignment and anatomical-alignment. For all results, statistical significance is set to be P-value  $< 0.05$ .

#### **Results**

The mean and standard deviation for the phase values of bilateral thalamus zero-alignment and anatomical alignment groups are summarized in (Table 1).

In both zero-alignment and anatomical-alignment, the filtered phase values in the anatomical alignment were significantly lower in negativity than those in the zero-alignment in bilateral thalamus ( $P < 0.05$ ) (Table 2).

The global mean of the zero-alignment group for the bilateral Thalamus was -10.6806 milli radians, versus -6.8246 milli radians for the anatomical-alignment group, the phase change is about -3.856 milli radians (56.5%) with P-value of =0.000.

**TABLE 1. Mean Phase values for each ROI of all patients.**

Deep gray matter regions in different alignments		Mean m. radians	Std. Deviation
LT Thalamus	Anatomical-Alignment	-3.39870	1.734905
	zero-alignment	-5.00940	2.486178
RT Thalamus	Anatomical-Alignment	-3.26190	1.764525
	zero-alignment	-5.83520	3.890113

**TABLE 2. Comparison between the two alignment groups of phase values ( $x \pm SD$ ) with a significance value of p-value and the value of t-test.**

Deep gray matter regions in different alignments		Mean Difference	Std. Deviation	t	P-Value
LT Thalamus	Zero alignment-anatomical alignment	-1.610700	1.681588	-3.029	0.014
RT Thalamus	Zero alignment-anatomical alignment	-2.573300	2.647629	-3.074	0.013

## Discussion

When applied to a high field MRI scanner, the SWI phase increases sensitivity to deoxygenated blood, iron, myelin, and other variations in susceptibility [30, 31]. However, the magnetic field orientation and slab alignment with respect to the main magnetic field have a big impact on phase image characterization [32, 33]. With pure transverse slab imaging, early investigations on SWI and phase in the brain tended to maintain the longer voxel dimension oriented in parallel to the main magnetic field. [1, 34]. Most recent investigations, typically use standard clinical brain alignment along the AC-PC line [35-37], to match anatomic features between subjects as well as between imaging methods. The voxel alignment angle with the main magnetic field varies amongst patients as a result of this AC-PC line alignment. According to the anatomical position of the AC-PC line, the SWI images were acquired at angles ranging from +15 to -15 degrees in this investigation. Several factors influence SWI phase measurements in the thalamus, including the ROI selection method, field strength, sample size, and composition properties[38]. In these measurements, we applied the same ROI method, the same field strength of 1.5 tesla, and the same subject per comparative measurement, so any

phase change that has occurred will be the result of the change in imaging slab volume orientation.

As in the results, the global mean of the zero-alignment group was (56.5%) more negative than the results of the anatomical-alignment group, which leads to a decrease in quantitative and qualitative measurements for subjects undergoing SWI in the anatomical orientation.

Our results showed that there was appreciable phase change for the thalamus in both hemispheres; between the two alignment groups. The mean phase values of the thalamus in the left and right hemispheres of the zero-alignment group were stronger (more negative) than those in the anatomical alignment group.

For bilateral hemispheres of the thalamus, there were significant differences between the two image groups ( $P < 0.05$ ). Student T-test results of -3 signify the large relative difference between the two groups.

Our results coincide with Eissa and Walsh [27, 39] respectively; where Eissa has measured the contrast to noise ratio (CNR) of SWI by comparing the pure axial and the oblique, at 45° degrees with his technique. Three-dimensional MRI with independent slab excitation and encoding (ISEE),

the results showed that the pure axial of SWI and SWI of ISEE had higher CNR than that of the SWI oblique.

Zero-alignment measurements give the best results to increase the sensitivity to phase variation due to paramagnetic depositions, owing to the strong reliance of phase images on voxel alignment with the main magnetic field. This could be arising from the fact that a dipole source has external and nonlocal field effects of variable signs that depend on the angle with the main magnetic field. Voxels aligned parallel to the main field lead to a different phase summation than that when voxels are not parallel [25, 28]. These effects will vary with voxel size, object shape, and voxel anisotropy[26]. By using small isotropic voxels, it can reduce the effects of voxel orientation, but would require a much longer acquisition time[26] in addition to having lower phase contrast.

Future work is warranted to increase the sample size and investigate the angle value effect on phase and contrast in a closer manner.

### **Conclusion**

Due to the substantial reliance of phase image on voxel alignment with the main magnetic field, acquiring SWI in a pure axial plan yields the best results in phase value, which enhances sensitivity to phase variation due to paramagnetic depositions. SWI images of the Thalamus gave higher contrast and phase effects due to iron content. By maintaining the imaging angle at pure axial, we may secure phase effects that are significantly (56.5%), P-value= 0.000 stronger than the standard anatomically based alignment. After being acquired in zero alignments, SWI pictures can be reconstructed in the desired anatomical alignment.

### *Data availability*

The data that support the findings of this study are available on request from the corresponding author.

### *Conflict of interest*

The authors declare no conflict of interest.

### **References**

- Haacke, E. M., Xu, Y., Cheng, Y. C. N., & Reichenbach, J. R. (2004). Susceptibility weighted imaging (SWI). *Magn Reson Med*, 52(3), 612-618. doi:10.1002/mrm.20198
- Liu, C., Li, W., Tong, K. A., Yeom, K. W., & Kuzminski, S. (2015). Susceptibility-weighted imaging and quantitative susceptibility mapping in the brain. *J Magn Reson Imaging*, 42(1), 23-41. doi:10.1002/jmri.24768
- Haacke, E. M., Mittal, S., Wu, Z., Neelavalli, J., & Cheng, Y. C. (2009). Susceptibility-weighted imaging: technical aspects and clinical applications, part 1. *AJNR Am J Neuroradiol*, 30(1), 19-30. doi:10.3174/ajnr.A1400
- Schweser, F., Deistung, A., Lehr, B. W., & Reichenbach, J. R. (2011). Quantitative imaging of intrinsic magnetic tissue properties using MRI signal phase: an approach to in vivo brain iron metabolism? *Neuroimage*, 54(4), 2789-2807. doi:10.1016/j.neuroimage.2010.10.070
- Ward, R. J., Zucca, F. A., Duyn, J. H., Crichton, R. R., & Zecca, L. (2014). The role of iron in brain ageing and neurodegenerative disorders. *Lancet Neurol*, 13(10), 1045-1060. doi:10.1016/s1474-4422(14)70117-6
- Li, K., & Reichmann, H. (2016). Role of iron in neurodegenerative diseases. *J Neural Transm (Vienna)*, 123(4), 389-399. doi:10.1007/s00702-016-1508-7
- Hagemeyer, J., Geurts, J. J., & Zivadinov, R. (2012). Brain iron accumulation in aging and neurodegenerative disorders. *Expert Rev Neurother*, 12(12), 1467-1480. doi:10.1586/ern.12.128
- Kruer, M. C. (2013). The neuropathology of neurodegeneration with brain iron accumulation. *Int Rev Neurobiol*, 110, 165-194. doi:10.1016/b978-0-12-410502-7.00009-0
- Pitt, D., Boster, A., Pei, W., Wohleb, E., Jasne, A., Zachariah, C. R., . . . Schmalbrock, P. (2010). Imaging cortical lesions in multiple sclerosis with ultra-high-field magnetic resonance imaging. *Arch Neurol*, 67(7), 812-818. doi:10.1001/archneurol.2010.148
- Drayer, B., Burger, P., Hurwitz, B., Dawson, D., & Cain, J. (1987). Reduced signal intensity on MR images of thalamus and putamen in multiple sclerosis: increased iron content? *AJR Am J Roentgenol*, 149(2), 357-363. doi:10.2214/ajr.149.2.357
- Mittal, S., Wu, Z., Neelavalli, J., & Haacke, E. M. (2009). Susceptibility-weighted imaging: technical aspects and clinical applications, part 2. *AJNR Am J Neuroradiol*, 30(2), 232-252. doi:10.3174/ajnr.A1461

12. Abosch, A., Yacoub, E., Ugurbil, K., & Harel, N. (2010). An assessment of current brain targets for deep brain stimulation surgery with susceptibility-weighted imaging at 7 tesla. *Neurosurgery*, 67(6), 1745-1756; discussion 1756. doi:10.1227/NEU.0b013e3181f74105
13. Behrens, T. E., Johansen-Berg, H., Woolrich, M. W., Smith, S. M., Wheeler-Kingshott, C. A., Boulby, P. A., . . . Matthews, P. M. (2003). Non-invasive mapping of connections between human thalamus and cortex using diffusion imaging. *Nat Neurosci*, 6(7), 750-757. doi:10.1038/nn1075
14. Saalman, Y. B., & Kastner, S. (2011). Cognitive and perceptual functions of the visual thalamus. *Neuron*, 71(2), 209-223. doi:10.1016/j.neuron.2011.06.027
15. Byne, W., Hazlett, E. A., Buchsbaum, M. S., & Kemether, E. (2009). The thalamus and schizophrenia: current status of research. *Acta Neuropathol*, 117(4), 347-368. doi:10.1007/s00401-008-0404-0
16. Haacke, E. M., Makki, M., Ge, Y., Maheshwari, M., Sehgal, V., Hu, J., . . . Grossman, R. I. (2009). Characterizing iron deposition in multiple sclerosis lesions using susceptibility weighted imaging. *J Magn Reson Imaging*, 29(3), 537-544. doi:10.1002/jmri.21676
17. Louis, E. D., & Ferreira, J. J. (2010). How common is the most common adult movement disorder? Update on the worldwide prevalence of essential tremor. *Mov Disord*, 25(5), 534-541. doi:10.1002/mds.22838
18. Tuleasca, C., Najdenovska, E., Régis, J., Witjas, T., Girard, N., Champoudry, J., . . . Van De Ville, D. (2018). Pretherapeutic Motor Thalamus Resting-State Functional Connectivity with Visual Areas Predicts Tremor Arrest After Thalamotomy for Essential Tremor: Tracing the Cerebello-thalamo-visuo-motor Network. *World Neurosurg*, 117, e438-e449. doi:10.1016/j.wneu.2018.06.049
19. Elias, W. J., Lipsman, N., Ondo, W. G., Ghanouni, P., Kim, Y. G., Lee, W., . . . Chang, J. W. (2016). A Randomized Trial of Focused Ultrasound Thalamotomy for Essential Tremor. *N Engl J Med*, 375(8), 730-739. doi:10.1056/NEJMoa1600159
20. Santos, A. G., da Rocha, G. O., & de Andrade, J. B. (2019). Occurrence of the potent mutagens 2-nitrobenzanthrone and 3-nitrobenzanthrone in fine airborne particles. *Sci Rep*, 9(1), 1. doi:10.1038/s41598-018-37186-2
21. Vérard, L., Allain, P., Travère, J. M., Baron, J. C., & Bloyet, D. (1997). Fully automatic identification of AC and PC landmarks on brain MRI using scene analysis. *IEEE Trans Med Imaging*, 16(5), 610-616. doi:10.1109/42.640751
22. Bernstein, M. A., & Licato, P. E. (1994). Angle-dependent utilization of gradient hardware for oblique MR imaging. *J Magn Reson Imaging*, 4(1), 105-108. doi:10.1002/jmri.1880040121
23. Schäfer, A., Wharton, S., Gowland, P., & Bowtell, R. (2009). Using magnetic field simulation to study susceptibility-related phase contrast in gradient echo MRI. *Neuroimage*, 48(1), 126-137. doi:10.1016/j.neuroimage.2009.05.093
24. Marques, J. P., Maddage, R., Mlynarik, V., & Gruetter, R. (2009). On the origin of the MR image phase contrast: an in vivo MR microscopy study of the rat brain at 14.1 T. *Neuroimage*, 46(2), 345-352. doi:10.1016/j.neuroimage.2009.02.023
25. Deistung, A., Rauscher, A., Sedlacik, J., Stadler, J., Witoszynskyj, S., & Reichenbach, J. R. (2008). Susceptibility weighted imaging at ultra high magnetic field strengths: theoretical considerations and experimental results. *Magn Reson Med*, 60(5), 1155-1168. doi:10.1002/mrm.21754
26. Xu, Y., & Haacke, E. M. (2006). The role of voxel aspect ratio in determining apparent vascular phase behavior in susceptibility weighted imaging. *Magn Reson Imaging*, 24(2), 155-160. doi:10.1016/j.mri.2005.10.030
27. Walsh, A., Wieler, M., Martin, W., & Wilman, A. (2010). Susceptibility phase imaging of the basal ganglia: Effects of phase filtering, slice orientation and ROI selection with comparison to T2\* mapping. *Proceedings of the 18th Annual Meeting of ISMRM*.
28. Sedlacik, J., Rauscher, A., & Reichenbach, J. R. (2007). Obtaining blood oxygenation levels from MR signal behavior in the presence of single venous vessels. *Magn Reson Med*, 58(5), 1035-1044. doi:10.1002/mrm.21283
29. Schneider, C. A., Rasband, W. S., & Eliceiri, K. W. (2012). NIH Image to ImageJ: 25 years of image analysis. *Nat Methods*, 9(7), 671-675. doi:10.1038/nmeth.2089
30. Bai, X., Wang, G., Wu, L., Liu, Y., Cui, L., Shi, H., & Guo, L. (2014). Deep-gray nuclei susceptibility-weighted imaging filtered phase shift in patients with Wilson's disease. *Pediatr Res*, 75(3), 436-442. doi:10.1038/pr.2013.239

31. Haacke, E. M., Xu, Y., Cheng, Y. C. N., & Reichenbach, J. R. (2004). Susceptibility weighted imaging (SWI). *Magnetic Resonance in Medicine: An Official Journal of the International Society for Magnetic Resonance in Medicine*, 52(3), 612-618.
32. Schäfer, A., Wharton, S., Gowland, P., & Bowtell, R. (2009). Using magnetic field simulation to study susceptibility-related phase contrast in gradient echo MRI. *Neuroimage*, 48(1), 126-137.
33. Sato, R., Shirai, T., Taniguchi, Y., Murase, T., Bito, Y., Soutome, Y., & Ochi, H. (2018). Susceptibility difference weighted imaging in vertical-field MRI. *Radiol Phys Technol*, 11(2), 255-261. doi:10.1007/s12194-018-0458-1
34. Reichenbach, J. R., Venkatesan, R., Schillinger, D. J., Kido, D. K., & Haacke, E. M. (1997). Small vessels in the human brain: MR venography with deoxyhemoglobin as an intrinsic contrast agent. *Radiology*, 204(1), 272-277.
35. Ngo, G. C., Wong, C. N., Guo, S., Paine, T., Kramer, A. F., & Sutton, B. P. (2017). Magnetic susceptibility induced echo time shifts: Is there a bias in age related fMRI studies? *Journal of Magnetic Resonance Imaging*, 45(1), 207-214.
36. McDannold, N., White, P. J., & Cosgrove, G. R. (2020). Using phase data from MR temperature imaging to visualize anatomy during MRI-guided focused ultrasound neurosurgery. *IEEE Transactions on Medical Imaging*, 39(12), 3821-3830.
37. Liu, Y., Wang, G., Zhao, L., Geng, M., Wang, L., Bai, X., ... Man, X. (2013). SWI phase asymmetries in deep gray matter of healthy adults: is there an association with handedness? *Brain imaging and behavior*, 7(2), 220-226.
38. Pfefferbaum, A., Adalsteinsson, E., Rohlfing, T., & Sullivan, E. V. (2009). MRI estimates of brain iron concentration in normal aging: comparison of field-dependent (FDRI) and phase (SWI) methods. *Neuroimage*, 47(2), 493-500. doi:10.1016/j.neuroimage.2009.05.006
39. Eissa, A., & Wilman, A. H. (2012). Three-dimensional MRI with independent slab excitation and encoding. *Magn Reson Med*, 67(2), 484-489. doi:10.1002/mrm.23043

#### تأثير توجهات الشريحة على الصور المرجحة بالحساسية الخاصة بالمهاد

محمود رفعت<sup>1</sup>، أمير عيسى<sup>1</sup>، محمد السماحي<sup>2</sup> و تامر محمود السيد<sup>1</sup>  
<sup>1</sup>شعبة الفيزياء الحيوية، قسم الفيزياء، كلية العلوم، جامعة الأزهر، مدينة نصر، القاهرة،  
<sup>2</sup>قسم جراحة المخ والأعصاب، كلية الطب، جامعة قناة السويس- مصر.

المهاد هو بنية دماغية تحت القشرية تنقسم إلى نوى أصغر ذات وظائف محددة تساعد في نقل الإشارات العصبية وتنظيمها، وقد كان موضوعاً للعديد من الدراسات العصبية والعلاجات السريرية، كما أن طرق التصوير التقليدية مثل التصوير الموزون T1 و T2 توفر تبايناً ضعيفاً في المهاد. يعتبر المهاد هدف واعد للصورة المرجحة بالحساسية الذي هو عبارة عن صورته من تسلسل صدى متدرج، وهو حساس للغاية للمركبات ذات الخصائص المغناطيسية. يمكن أن تساعد طور وقيمة الصور المرجحة بالحساسية في تشخيص مجموعة متنوعة من الأمراض. الاختلافات المكانية في المجال المغناطيسي الأساسي لجهاز التصوير بالرنين المغناطيسي لها تأثير كبير على البيانات الخاصة بالطور. عند الحصول على الصور المرجحة بالحساسية في التصوير التشخيصي، يكون المحاذاة المحورية هو المستوى الأكثر شيوعاً للمحاذاة. بسبب عدم التجانس النسبي في وضع المريض والوضع التشريحي للمخ، غالباً ما تؤدي المتطلبات السريرية إلى تغييرات في زوايا المحاذاة. يمكن أن يتغير خط الصور الأمامي والخلفي في الاتجاه فيما يتعلق بالمستوى العرضي لنظام التصوير بالرنين المغناطيسي للعديد من المرضى الذين يتلقون التصوير بالرنين المغناطيسي للدماغ. درسنا ما إذا كانت هناك أي تأثيرات كبيرة على بيانات الطور الخاصة بالصور المرجحة بالحساسية بسبب الاتجاه المائل. وفقاً للبيانات الناتجة، كانت هناك تغييرات كبيرة في قيم الطور بين الحالات المحورية والمحاذاة تشريحياً.